Since January 2020 Elsevier has created a COVID-19 resource centre with free information in English and Mandarin on the novel coronavirus COVID-19. The COVID-19 resource centre is hosted on Elsevier Connect, the company's public news and information website.

Journal Pre-proof

Tropism of SARS-CoV-2 for Barrett's Esophagus may Increase Susceptibility to Developing COVID-19

Ramon U. Jin, M.D., Ph.D., Jeffrey W. Brown, M.D., Ph.D., Qing Kay Li, M.D., Ph.D., Peter O. Bayguinov, Ph.D., Jean S. Wang, M.D., Ph.D., Jason C. Mills, M.D., Ph.D., Collaborators, Sean P.J. Whelan, Ph.D., James A.J. Fitzpatrick, Ph.D., Alan K. Meeker, MAT, Ph.D.

PII: S0016-5085(21)00091-3
DOI: https://doi.org/10.1053/j.gastro.2021.01.024
Reference: YGAST 64051

To appear in: *Gastroenterology*
Accepted Date: 10 January 2021

Please cite this article as: Jin RU, Brown JW, Li QK, Bayguinov PO, Wang JS, Mills JC, Collaborators, Whelan SPJ, Fitzpatrick JAJ, Meeker AK, Tropism of SARS-CoV-2 for Barrett's Esophagus may Increase Susceptibility to Developing COVID-19, *Gastroenterology* (2021), doi: https://doi.org/10.1053/j.gastro.2021.01.024.

Tropism of SARS-CoV-2 for Barrett's Esophagus may Increase Susceptibility to Developing COVID-19

Ramon U. Jin, M.D., Ph.D.[1, *]
Jeffrey W. Brown, M.D., Ph.D.[2,*†]
Qing Kay Li, M.D., Ph.D.[3]
Peter O. Bayguinov, Ph.D.[4]
Jean S. Wang, M.D., Ph.D.[2]
Jason C. Mills, M.D., Ph.D. [2,5,6 †]

[1] Division of Oncology, Department of Medicine, Washington University in St. Louis, School of Medicine, St. Louis, MO 63110 USA
[2] Division of Gastroenterology, Department of Medicine, Washington University in St. Louis, School of Medicine, St. Louis, MO 63110 USA
[3] Department of Pathology, Johns Hopkins Medical Institutions, Baltimore, MD, United States.
[4] Washington University Center for Cellular Imaging, Washington University School of Medicine, St. Louis, MO 63110, USA
[5] Department of Pathology and Immunology, Washington University in St. Louis, School of Medicine, St. Louis, MO 63110 USA
[6] Department of Developmental Biology, Washington University in St. Louis, School of Medicine, St. Louis, MO 63110 USA

[†]Correspondence should be addressed to:

Jeffrey W. Brown, M.D., Ph.D.
Washington University in St. Louis, School of Medicine
660 S. Euclid Avenue, Campus Box 8124
St. Louis, MO 63110
Email: brownjw@wustl.edu

or

Jason C. Mills, M.D., Ph.D.
Washington University in St. Louis, School of Medicine
660 S. Euclid Avenue, Campus Box 8124
St. Louis, MO 63110
Email: jmills@wustl.edu

Conflicts of Interest: None.

Contributions: RUJ, JWB, and JCM: Study Concept and Design, Acquisition of Data, Analysis and Interpretation of Data, Drafting the manuscript, Obtained Funding; QKL,

POB: Acquisition of Data; JSW: Provided essential resources

Running Title: Foregut Metaplasia and SARS-CoV-2

Keywords: Barrett's Esophagus, Intestinal Metaplasia of the Stomach, COVID, SARS-CoV-2, Organoid

Abbreviations used in this paper: IM: Intestinal Metaplasia; VSV: vesicular stomatitis virus; eGFP: enhanced Green Fluorescent Protein, COVID-19: Corona Virus Disease 2019; SARS-CoV-2: Severe Acute Respiratory Syndrome-related Coronavirus; ACE2: Angiotensin-Converting Enzyme 2; TMPRSS2: Transmembrane Protease, Serine 2; BSL-2: Biosafety Level 2; rVSV: recombinant vesicular stomatitis virus.

Collaborators:

Sean P.J. Whelan, Ph.D.[7]
[7] Department of Molecular Microbiology, Washington University School of Medicine, St. Louis, MO 63110 USA

James A.J. Fitzpatrick, Ph.D.[8,9,10]
[8] Washington University Center for Cellular Imaging, Washington University School of Medicine, St. Louis, MO 63110, USA
[9] Departments of Neuroscience and Cell Biology & Physiology, Washington University School of Medicine, St. Louis, MO 63110, USA
[10] Department of Biomedical Engineering, Washington University in St. Louis, St. Louis, MO 63110, USA

Alan K. Meeker, MAT, Ph.D.[3]
[3] Department of Pathology, Johns Hopkins Medical Institutions, Baltimore, MD, United States.

Words: 981

ACKNOWLEDGEMENTS

JWB acknowledges support from the American Gastroenterological Association Foundation AGA-Takeda COVID-19 Rapid Response Research Award AGA2021-5101, Department of Defense, through the PRCRP program under Award No. W81XWH-20-1-0630. POB and JAJF gratefully acknowledge support from the Washington University Center for Cellular Imaging, which is supported by Washington University School of Medicine, the Children's Discovery Institute of Washington University and St. Louis

Children's Hospital (CDI-CORE-2015-505 and CDI-CORE-2019-813), the Foundation for Barnes-Jewish Hospital (3770 and 4642) and the Alvin J. Siteman Cancer Center at Barnes-Jewish Hospital and Washington University School of Medicine (P30 CA091842). The authors thank the Advanced Imaging and Tissue Analysis Core of the Washington University Digestive Disease Research Core Center P30 DK052574 and the Oncology Tissue Core at JHU P30 CA006973. RUJ thanks support from T32HL007088. RUJ and JCM thank the BETRNet (NCI U54CA163060). JCM thanks support from R21DK111369, R01DK105129, and R01DK110406.

Introduction

COVID-19, caused by SARS-CoV-2, is a global pandemic, spurring exigent need for determining how the virus is transmitted and what increases disease susceptibility. Gastrointestinal (GI) symptoms are prominent in COVID-19, and live virus is detected along the GI tract and in stool[1]. SARS-CoV-2 enters host cells via its transmembrane spike glycoproteins that bind host ACE2 protein on the cell surface, an interaction facilitated by spike protein cleavage catalyzed by host type II transmembrane serine protease TMPRSS2[2]. Thus, concurrent cellular expression of ACE2 and TMPRSS2 determines cellular tropism for SARS-CoV-2. Surveys of ACE2 and TMPRSS2 in GI tissues have shown abundant expression in human intestines[3]. However, the low pH of gastric secretions[4] as well as emulsifying conditions[3] of the small and large intestinal inactivate the virus, limiting access of infective virus to distal GI tissues via the GI tract lumen. Here, we show that individuals with intestinal metaplasia (i.e. ectopic intestine-like cells in their esophagus as in Barrett's esophagus) would have increased potential for viable, ingested virus to interact with a receptive host epithelium. Thus, intestinal metaplasia could present a previously unappreciated orogastric route for viral entry in individuals with this condition.

Methods

All human tissue blocks were collected from the archives of The Johns Hopkins School of Medicine Bayview Medical Campus Department of Pathology. Barrett's esophagus organoids were derived from de-identified tissue from patients who were undergoing surveillance esophagogastroduodenoscopy for previously identified non-dysplastic

Barrett's esophagus and provided informed consent through the Washington University School of Medicine Digestive Disease Research Core Center. Human tissue collection was approved by Review Boards of each institution. Organoid cultures were infected with a chimeric virus expressing the SARS-CoV-2 spike protein (rVSV-eGFP-SARS-CoV-2). Both fixed and live cells were imaged by light, epifluorescence, and live confocal microscopy.

Results

To test whether intestinal-type metaplasias of the proximal GI foregut might be receptive to SARS-CoV-2 infection, we determined ACE2 and TMPRSS2 expression in a series of esophageal and gastric biopsies harboring intestinal metaplasia (Table S1). Unlike normal esophageal and gastric tissue, intestinal-type metaplasia of the esophagus and stomach strongly expressed both ACE2 and TMPRSS2 on epithelial cells with ACE2 predominantly localized to the apical plasma membranes (Fig. 1A; Table S1). The findings were corroborated by analyses of previous global surveys of RNA expression[e.g. 5] showing that unlike normal esophageal and gastric tissue, intestinal-type metaplasias of these tissues aberrantly express *ACE2* and *TMPRSS2* mRNA.

To test whether Barrett's metaplasia is susceptible to infection by SARS-CoV-2, we chose an *ex vivo* model: organoids derived from patients with Barrett's esophagus. We first demonstrate that organoids generated from biopsies of Barrett's esophagus faithfully reproduce the *in vivo* histopathologic characteristics (Fig. S1B). Specifically, they form a columnar monolayer that is low in expression of the foregut transcription

factor SOX2, high in expression of the mid and hindgut transcription factor CDX2, reactive to the histochemical goblet cell mucin stain Alcian blue and, importantly for this study, maintain the apical expression of ACE2 and TMPRSS2 (Fig. 1B; S1B,C).

We incubated three Barrett's esophageal organoid lines (WU014, WU002, and WU012) harboring unique intestinal characteristics (Fig. S1B) with a chimeric virus (rVSV-eGFP-SARS-CoV-2) in which the SARS-CoV-2 spike protein replaces the VSV glycoprotein G, and the eGFP gene is carried within viral RNA to report on intracellular translation of viral proteins. Thus, this chimeric virus exhibits the same tropism and cell invasion behavior of actual SARS-CoV-2 but can be studied in a BSL-2 facility. rVSV-eGFP-SARS-CoV-2 infected cells within 12 hours, and GFP signal, indicating active translation of viral RNA, persisted until our last time point 2 weeks later (Fig. 1C, D; Fig. S1D). We observed in an initial experiment (Experiment 1, Fig. 1D) that, while both patient organoid lines were efficiently infected, the line with increased intestinalization (i.e. lower SOX2 to CDX2 ratio, Fig. S1B) was more extensively infected. We thus repeated the experiment (Experiment 2; Fig. 1D) but added an additional line (WU0014) featuring even greater intestinal features (Fig. S1B). In Experiment 2, we also reasoned virus in patients would encounter intact epithelium, so we scored only those infected cells within organoids above a threshold size. Together, these organoid results show that Barrett's esophagus may serve as a novel *in vivo* niche for SARS-CoV-2, and that viral entry may increase with increasing intestinalization (Fig.1D).

Discussion

Esophageal and gastric metaplasia are caused by chronic injury and predispose individuals to developing adenocarcinoma of the respective tissue[6,7]; however, the data presented here suggest that these metaplasias may also have other unanticipated consequences.

We show that intestinal-type metaplasia of the esophagus and stomach aberrantly express the proteins critical for binding and invasion by SARS-CoV-2: ACE2 and TMPRSS2. Recent studies have demonstrated that the low pH of the stomach as well as the luminal fluid of the small intestine and large intestine greatly attenuate the infectivity of SARS-CoV-2 that is present in swallowed oral secretions and refluxed respiratory sputum[3,4]. Thus, the ectopic, proximal expression of ACE2 and TMPRSS2 may become salient as it means host receptors for SARS-CoV-2 are located in a region of the digestive tract where higher viable viral titers exist following ingestion. Moreover, individuals with known Barrett's esophagus are almost universally treated with proton pump inhibitors and those with gastric intestinal metaplasia almost invariably have loss of acid secreting parietal cells[6,7]. Thus, the decreased ability for the stomach to produce acid either by pharmacologic inhibition or loss of acid-secreting cells may compound the risk due to increased gastric pH which could result in increased viral titers and prolonged exposure. In addition, epidemiologically, intestinal metaplasia increases with age and male sex, paralleling demographics of those most susceptible to COVID-19[8].

Previous work indicates viable virus infects cells via SARS-CoV-2 spike protein interaction with apical ACE2 receptor. Two factors in our cultures increased apical exposure of cells to virus: a) we administered virus immediately after passaging (ie after dissociating organoids to single cells exposing all cell surfaces); and b) as new Barrett's

organoids form, many wholly or partially orient “apical-out”, ie with cell apices exposed to the culture medium (Fig. 1B). Importantly, all three organoid lines had equivalent distribution of apical-out, basal-out, and hybrid orientations (data not shown) indicating orientation did not affect infectivity.

Overall, our data suggest that individuals with intestinal-type metaplasias of proximal gastrointestinal tract (e.g. Barrett’s esophagus, in particular) are potentially at higher risk for developing or experiencing a more severe presentation of COVID-19 relative to the general population. Future studies to determine the additional risk posed by ectopic proximal expression of ACE2 and TMPRSS2 should include: infection of a much broader panel of organoids of varying intestinal differentiation and, eventually, large-scale retrospective database analyses correlated with autopsy series to analyze COVID-19 outcome vs. viral load and extent of metaplasia.

REFERENCES

1. Xiao F*, et al.* Gastroenterology 2020; 158:1831-3.

2. Hoffman M, *et al*. Cell 2020; 181(2): 271-80.

3. **Zang R, Castro MFG,** *et al*. Sci Immunol 2020; 5(47): eabc3582.

4. **Zang R, Castro MFG**, *et al*. *BioRXiv* 2020.

5. di Pietro M, *et al*. Proc Natl Acad Sci 2012; 109(23): 9077-82.

6. Spechler SJ & Souza RF N Engl J Med 2014; 371(9): 836-45.

7. Amieva M & Peek RM Gastroenterology 2016; 150(1): 64-78.

8. Wu Z & McGoogan JM JAMA 2020; 323(13): 1239-42.

Author names in bold designate shared co-first authorship

FIGURE LEGENDS:

Figure 1. **Barrett's esophagus expresses ACE2 and TMPRSS2 and is readily infected by rVSV-eGFP-SARS-CoV-2**. (A) Human Barrett's esophagus immunohistochemistry shows expression of apical ACE2, the host receptor for the SARS-CoV-2 spike protein and TMPRSS2, the necessary protease. Insets highlighting individual goblet cells outlined in yellow with apical ACE2 and TMPRSS2 expression patterns. Normal esophagus does not express apical ACE2 or TMPRSS2. Scale bars 200 µm. 'BE' indicating area of Barrett's esophagus; 'NE' indicating adjacent area of normal squamous esophagus. (B) Barrett's organoids grow with various mixtures of 'apical-out' and 'basal-out' arrangements. Epifluorescence imaging of fixed organoids demonstrates apical ACE2 staining (green) and TMPRSS2 staining (green) with β-actin staining (red) highlighting the apical surface. Confocal imaging using an Airyscan detector in SR mode showing super-resolution co-localization of ACE2 (green) and TMPRSS2 (green) with apical β-actin (red); intracellular and luminal spaces highlighted. Scale bars 100 µm or as indicated. (C) Z-stack still image of live confocal microscopy of infected Barrett's organoids with raw optical section and three-dimensional reconstruction shown. Organoid outer surface marked by dotted line, and individual green infected cells are outlined with a solid line in each organoid showing diffuse cytoplasmic (arrow heads) and punctate vesicular GFP patterns. Scale bars 100 µm. (D) Incubation of Barrett's esophagus organoids (WU014 with mostly intestinal features, WU002 with mixed intestinal-gastric features, and WU012 with mostly gastric features;

see Supplemental Figure 1B) with rVSV-eGFP-SARS-CoV-2. Experiment 1: quantification of all intracellular punctate GFP foci in Barrett's organoids (n=2 independent cultures); Experiment 2: only GFP puncta within organoids > 10 µm scored (n=3-6 independent cultures) at specified time points for 2 weeks. Live-cell brightfield and fluorescence imaging of WU002 Barrett's organoids at timepoints indicated. Note: a single field of organoids is followed serially in each panel. Persistently infected (green from GFP translated from rVSV-eGFP-SARS-CoV-2 virus) cells are indicated at the day 13 time point (arrow heads). Scale bars 200 µm. p-values by two-tailed, paired Student's *t*-test (Experiment 1) and by ANOVA with Dunnett multiple comparison test to WU012 as control (Experiment 2) of Area Under Curve at each timepoint from first timepoint to day 5 (see Supplemental Methods).

SUPPLEMENTAL METHODS:

Human Sample Collection, Immunohistochemistry and Quantification

Formalin-fixed Paraffin-Embedded (FFPE) tissue blocks of esophagus (n=26) and stomach (n=5) were from The Johns Hopkins School of Medicine Bayview Medical Campus Department of Pathology with Institutional Review Board approval. FFPE blocks were cut into 4-μm sections, deparaffinized and rehydrated prior to incubation with primary antibodies.

For manual ACE2 immunostaining, heat-induced antigen retrieval was via a steamer using Antigen Unmasking Solution (H-3300, Vector Laboratories) with blocking of endogenous peroxidase and phosphatase (S2003, Dako). Anti-ACE2 (1:2000 dilution; Ab15348, Abcam) was detected by HRP-labeled anti-rabbit secondary antibody (PV6119, Leica Microsystems), visualized with 3,3′-Diaminobenzidine (D4293, Sigma-Aldrich), and counterstained with Mayer's hematoxylin. ACE2 auto staining used a Ventana Discovery Ultra autostainer (Roche Diagnostics) with antigen retrieval performed by Ventana Ultra CC1 buffer (#6414575001, Roche Diagnostics). Primary antibody was detected with anti-rabbit HQ detection system (#7017936001 and 7017812001, Roche), visualized with Chromomap DAB IHC detection kit (#5266645001, Roche) and counterstained with hematoxylin.

For TMPRSS2 immunostaining, auto staining was as above with anti-TMPRSS2 (1:12,000 dilution; Ab92323, Abcam) primary antibody detected with the same anti-rabbit HQ detection system (#7017936001 and 7017812001, Roche), visualized by Chromomap DAB IHC kit (#5266645001, Roche Diagnostics), and counterstained with hematoxylin.

ACE2 and TMPRSS2 staining were quantified in areas of Barrett's esophagus or gastric intestinal metaplasia through review of H&E histology. ACE2 and TMPRSS2 stained serial sections were scored: 0 = no apical staining; 1 = <50% of apical staining, 2 = >50% apical staining in 20x fields of view in areas of Barrett's esophagus or gastric intestinal metaplasia, and adjacent tissue controls when available.

Human Barrett's Esophagus Organoid Culture System

Barrett's esophagus organoids were derived from de-identified tissue from patients who were undergoing Barrett's esophagus surveillance esophagogastroduodenoscopy (EGD) for previously identified non-dysplastic Barrett's esophagus, approved by the Institutional Review Board of Washington University School of Medicine, and provided informed consent through the Washington University School of Medicine Digestive Disease Research Core Center. In brief, Barrett's esophagus organoids were cultured with L-WRN-conditioned media[1] supplemented with 10nM gastrin (Sigma-Aldrich), 10mM nicotinamide (Sigma-Aldrich), 500nM A83-01 (Tocris), 10µM SB202190 (Sigma-Aldrich), 200ng/mL FGF10 (Peprotech), 10µM Y-27632 (Sigma-Aldrich), and Primocin (Invivogen) in 3D Matrigel (Corning) in 24-well plates[2]. Organoids were expanded and passaged every 7-10 days (except for virus infection experiments, see below) by mechanical dissociation from matrigel, dispersed using TrypLE (Thermo Fisher) and manual pipetting, and transferred into new matrigel and plated in 24-well plates.

Human Barrett's Esophagus Organoid Immunofluorescence/Immunohistochemical Staining

Human Barrett's esophagus organoids were pelleted and fixed in 10% formalin at 4C for one hour. Organoids were washed, moved to 70% ethanol, mounted in 3% agar and embedded in paraffin. Blocks were cut into 7-micron sections. For immunofluorescence, tissue microtome sections underwent a standard deparaffinization with xylene and rehydration protocol and were antigen retrieved in sodium citrate buffer (2.94 g sodium citrate, 500 uL Tween 20, pH 6.0) using a pressure cooker. Sections were blocked in 1% BSA, 0.3% Triton X-100 in PBS and incubated with primary antibodies: anti-ACE2 (1:100 dilution; catalog# Ab15348, Abcam), anti-TMPRSS2 (1:100 dilution; catalog# HPA035787, Sigma-Aldrich), and anti-β-Actin (1:200 dilution; catalog# A1978, Sigma-Aldrich). Fluorescent secondary antibodies were applied, and slides were mounted using ProLong Gold antifade reagent with DAPI (Molecular Probes). For

immunohistochemistry, the same manual staining procedure for anti-ACE2 staining and auto staining procedure for TMPRSS2 was used as described above.

Viral Infection of Human Barrett's Esophagus Organoids and Quantification

rVSV-eGFP-SARS-CoV-2 chimeric virus (eGFP reporter encoded in the viral RNA) was constructed by P.W. Rothlauf and S.P.J. Whelan using the SARS-CoV-2 Wuhan-Hu-1 spike and the VSV Indiana strain[3]. The virus was generated and recovered according to previous published methods[4], and propagated in MA104 cells (ATCC). Organoids were infected with $2.0x10^5$ PFU of infectious rVSV-eGFP-SARS-CoV-2 (MOI=0.5) for long-term infection assays or for 48 hours prior to live confocal imaging.

For long-term organoid viral quantification experiments, 75,000 Barrett's esophagus cells were seeded into 48-well plates prior to viral infections as described. Brightfield and fluorescent imaging was performed using the BioTek Lionheart Cell Imaging Multi-mode Reader as described below every 12 hours for 312 hours total or every day for 14 days. Visible green punctae per well were counted for Experiment 1 and visible green puncta in organoids larger than 10 µm were counted for Experiment 2. These data were then graphed and analyzed using GraphPad Prism 8.1.1. For statistical analysis that incorporated the repeated, sequential measures of the same cultures over time, data were transformed by measuring AUC (Area Under the Curve) for each time point until day 5 (the timepoint in both experiments when peak viral entry returned towards a steady-state, baseline in all organoid lines). Statistical significance was calculated from the transformed data (ie the AUC calculations). For the two organoid lines in Experiment 1 a paired two tailed Student's *t*-test was used. Statistical significance for Experiment 2 was calculated using paired ANOVA of mean AUC values with *post hoc* Dunnett correction where WU012 was considered the control. Alpha was 0.05 for all approaches.

Imaging

Fluorescence microscopy was performed using a Zeiss Axiovert 200 microscope with an Axiocam MRM camera and Apotome II instrument for grid-based optical sectioning. Immunofluorescence images were taken on a Zeiss Apotome (Zeiss). Bright field images were taken on an Olympus BX43 light microscope. Long-term infection organoid fluorescent imaging was performed on a BioTek Lionheart Cell Imaging Multi-mode Reader. Live confocal imaging was performed at the Washington University Center for Cellular Imaging using a Zeiss LSM880 Confocal Microscope with Airyscan unit and Pecon stage-top incubator. Images were analyzed and post-imaging adjustments were performed with Adobe Photoshop CS6, and line art was generated in Adobe Illustrator CS6.

REFERENCES:

1. VanDussen KL, Sonnek NM, Stappenbeck TS: L-WRN conditioned medium for gastrointestinal epithelial stem cell culture shows replicable batch-to-batch activity levels across multiple research teams. Stem Cell Res 37:101430, 2019
2. Sato T, Stange DE, Ferrante M, et al: Long-term expansion of epithelial organoids from human colon, adenoma, adenocarcinoma, and Barrett's epithelium. Gastroenterology 141:1762-72, 2011
3. Case JB, Rothlauf PW, Chen RE, et al: Neutralizing Antibody and Soluble ACE2 Inhibition of a Replication-Competent VSV-SARS-CoV-2 and a Clinical Isolate of SARS-CoV-2. Cell Host Microbe 28:475-485 e5, 2020
4. Whelan SP, Ball LA, Barr JN, et al: Efficient recovery of infectious vesicular stomatitis virus entirely from cDNA clones. Proc Natl Acad Sci U S A 92:8388-92, 1995

Supplemental Figure 1. **Gastric intestinal metaplasia expresses ACE2 and TMPRSS2; additional characterization of Barrett's esophagus organoids**. (A) Immunohistochemistry of human gastric intestinal metaplasia ('GIM') and adjacent stomach ('Stom') shows apical expression of ACE2 and TMPRSS2. Small intestine staining for both proteins shown as a positive control. Insets highlighting individual goblet cells outlined in yellow with apical ACE2 and TMPRSS2 expression patterns. Scale bars 200 µm. (B) H&E images demonstrating the distinct columnar epithelium morphology and immunohistochemical staining of SOX2 (brown nuclear pattern), CDX2 (brown nuclear pattern), and Alcian blue (blue vesicular cytoplasmic pattern) for three human Barrett's esophagus organoid lines (WU014, WU002 and WU012). Scale bars 100 µm. (C) Immunohistochemical staining of ACE2 (brown apical cytoplasmic) and TMPRSS2 (brown diffuse cytoplasmic) for the intestinal WU002 human Barrett's esophagus organoid line. Scale bars 100 µm. (D) Three-dimensional confocal Z-stack series ("top" of the organoid to the "bottom") with Airyscan detector used as indicated of live Barrett's organoids infected with rVSV-eGFP-SARS-CoV-2 demonstrating diffuse cytoplasmic (arrow heads) and punctate vesicular green GFP patterns. The organoid lumen and outer surface are marked by dotted line. An example, individual infected cells are outlined with a solid line in each organoid. Individual green infected cells are outlined with a solid line in each organoid showing diffuse cytoplasmic (arrow heads) and punctate vesicular GFP patterns. Scale bars 100 µm.

Supplemental Table 1. **Barrett's esophagus and Gastric Intestinal Metaplasia express ACE2 and TMPRSS2**. Patient age, sex, protein pump inhibitor (PPI) use,

biopsy location (Esophagus, Gastroesophageal junction, Stomach), pathologic diagnosis, and quantification of ACE2 and TMPRSS2 immunohistochemical staining in human tissue specimens of Barrett's esophagus (Barrett's without dysplasia, Barrett's with Low-grade dysplasia, Barrett's with High-grade dysplasia) and gastric intestinal metaplasia. Scoring system: 0 = no apical staining; 1 = <50% of apical staining, 2 = >50% apical staining in 20x fields of view in areas of Barrett's esophagus or gastric intestinal metaplasia, and adjacent tissue controls. Areas without adjacent tissue controls are marked with 'N/A'.

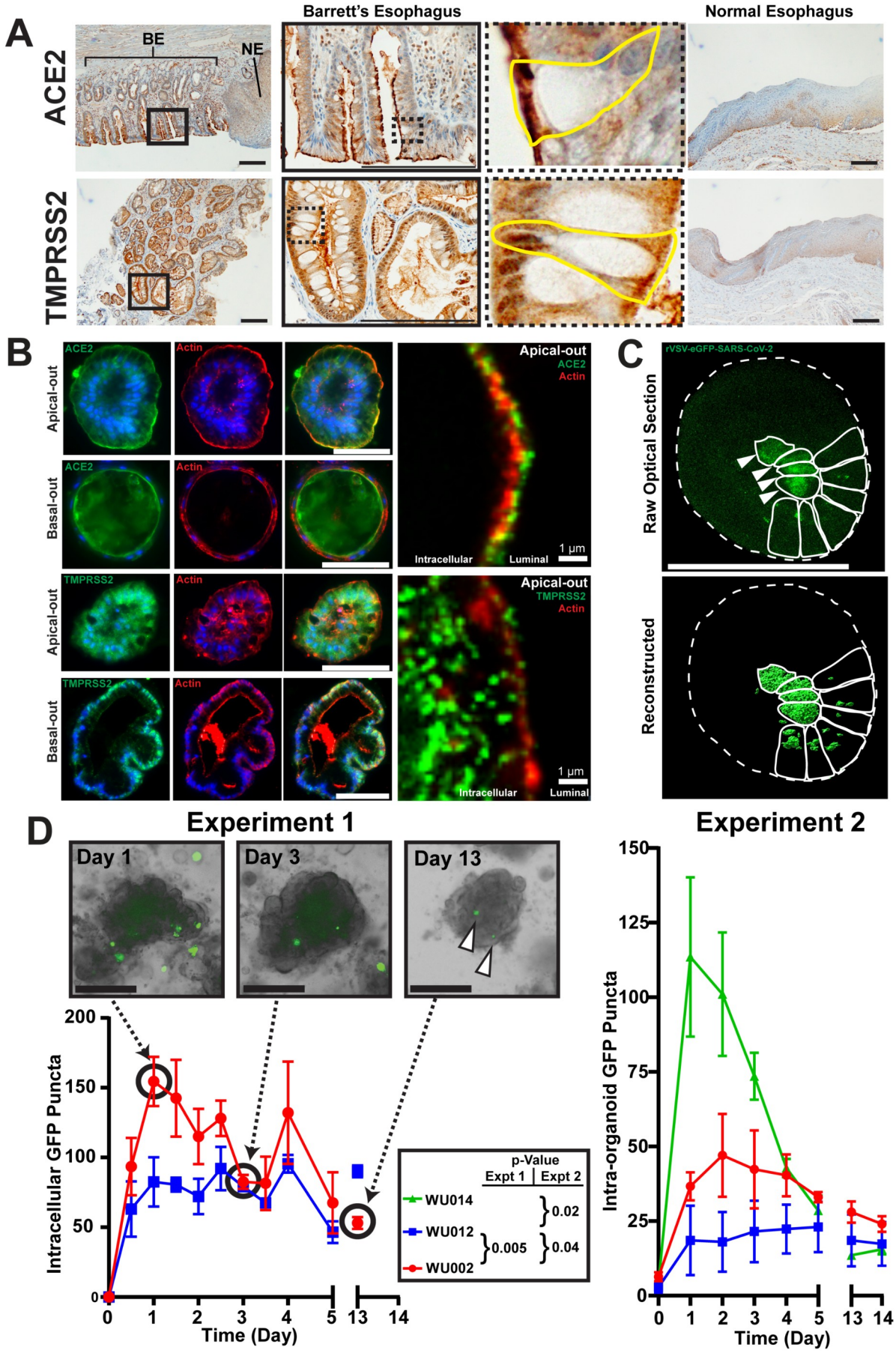
A
Barrett's Esophagus
Normal Esophagus
ACE2
TMPRSS2
BE
NE
B
Apical-out
Basal-out
ACE2
Actin
TMPRSS2
Intracellular
Luminal
1 µm
C
rVSV-eGFP-SARS-CoV-2
Raw Optical Section
Reconstructed
D
Experiment 1
Experiment 2
Day 1
Day 3
Day 13
Intracellular GFP Puncta
Intra-organoid GFP Puncta
Time (Day)
p-Value
Expt 1 | Expt 2
WU014
WU012
WU002
0.02
0.005
0.04

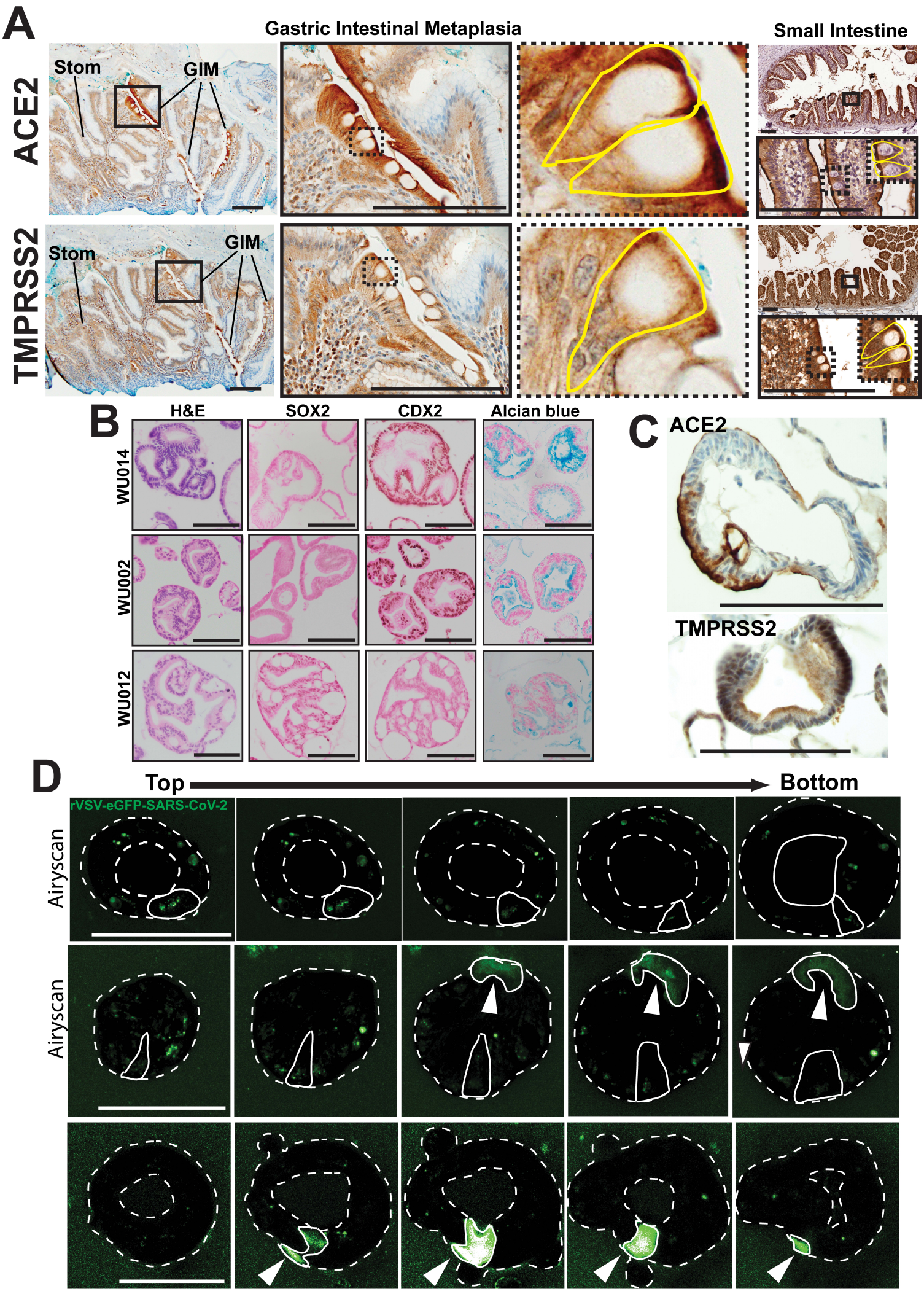
A
Gastric Intestinal Metaplasia
Small Intestine
ACE2
TMPRSS2
Stom
GIM
B
H&E
SOX2
CDX2
Alcian blue
WU014
WU002
WU012
C
ACE2
TMPRSS2
D
Top
Bottom
rVSV-eGFP-SARS-CoV-2
Airyscan
Airyscan

Age	Sex	PPI Use	Biopsy Location	Diagnosis	ACE2 Score (Metaplasia)	ACE2 Score (Adjacent Tissue)	TMPRSS2 Score (Metaplasia)	TMPRSS2 Score (Adjacent Tissue)
57	M	Yes	Esophagus	Barrett's without dysplasia	1	0	1	0
82	M	Yes	Esophagus	Barrett's without dysplasia	2	0	1	0
63	M	No	Esophagus	Barrett's without dysplasia	2	0	1	0
78	M	Yes	Esophagus	Barrett's without dysplasia	1	1	1	0
75	M	Yes	GE Junction	Barrett's without dysplasia	2	0	1	0
76	M	Yes	Esophagus	Barrett's without dysplasia	1	0	1	0
60	F	Yes	GE Junction	Barrett's without dysplasia	1	0	2	0
57	M	Yes	Esophagus	Barrett's without dysplasia	2	N/A	1	N/A
66	M	Yes	Esophagus	Barrett's without dysplasia	2	0	0	0
68	M	No	Esophagus	Barrett's without dysplasia	2	0	1	0
59	M	No	Esophagus	Barrett's without dysplasia	2	0	1	0
71	M	Yes	Esophagus	Barrett's without dysplasia	2	0	1	0
75	M	Yes	GE Junction	Barrett's without dysplasia	2	0	1	0
66	M	Yes	Esophagus	Barrett's with Low-grade dysplasia	2	N/A	1	N/A
84	M	Yes	Esophagus	Barrett's with Low-grade dysplasia	2	0	1	0
66	M	Yes	Esophagus	Barrett's with Low-grade dysplasia	2	0	2	0
54	F	Yes	Esophagus	Barrett's with High-grade dysplasia	2	0	1	0
67	M	Yes	Esophagus	Barrett's with High-grade dysplasia	2	0	2	0
71	M	No	Esophagus	Barrett's with High-grade dysplasia	2	0	1	0
60	M	No	Esophagus	Barrett's with High-grade dysplasia	1	0	1	0
53	M	Yes	GE Junction	Barrett's with High-grade dysplasia	2	0	2	0
60	F	Yes	GE Junction	Barrett's with High-grade dysplasia	2	0	2	0
78	M	Yes	Esophagus	Barrett's with High-grade dysplasia	2	0	1	0
60	F	No	Esophagus	Barrett's with High-grade dysplasia	2	0	1	0
65	M	No	Esophagus	Barrett's with High-grade dysplasia	2	0	1	0
51	M	No	Esophagus	Barrett's with High-grade dysplasia	2	0	2	0
54	M	Yes	Gastric	Intestinal Metaplasia	1	0	0	0
49	F	No	Gastric	Intestinal Metaplasia	2	0	1	0
73	M	Yes	Gastric	Intestinal Metaplasia	2	N/A	1	N/A
76	M	Yes	Gastric	Intestinal Metaplasia	2	0	1	0
69	M	No	Gastric	Intestinal Metaplasia	1	0	1	0